

Influence of Change in Ether Structure on the Low Temperature Dielectric Relaxation of Some Poly(ether imide)

Geoffrey C. Eastmond,¹ Jerzy Paprotny,¹ Richard A. Pethrick,² Fernan Santamaria-Mendia^{1,2}

¹Department of Chemistry, Donnan Laboratory, University of Liverpool, Liverpool L69 7ZD, United Kingdom

²WestCHEM, Department of Pure and Applied Chemistry, University of Strathclyde, G1 1XL Glasgow, United Kingdom

Correspondence to: R. A. Pethrick (E-mail: r.a.pethrick@strath.ac.uk)

ABSTRACT: Broad band dielectric relaxation spectra are reported on a range of polymers created by varying the ether segment in a series of poly(ether imide)s. Changes in the structure allow the effects of steric constraints on the local conformational dynamics of the polymer chain to be explored. These changes have a significant effect on the glass transition temperatures of these polymers which range from 245 to over 420°C. In contrast, the low temperature dielectric relaxation behavior of these polymers is very similar and is attributed to cooperative local oscillatory—librational motions. Changes in the stereochemistry effect the amplitude, activation energy for the relaxation process, the packing chain density, and values of the high frequency limiting permittivity, ϵ_{∞}' . This latter parameter is sensitive to the extent of dipole induced dipole and π - π electron interactions and is influenced by the packing density. The magnitude of ϵ_{∞}' is a very important parameter in determining the suitability of poly(imide)s for electrical applications. The magnitude of ϵ_{∞}' increases with the density; however, deviations from this general trend are observed when large nonpolar groups inhibit the interaction of neighboring chains. © 2014 Wiley Periodicals, Inc. *J. Appl. Polym. Sci.* **2014**, *131*, 41191.

KEYWORDS: dielectric properties; glass transition; polyimides; properties and characterization; property relations; structure

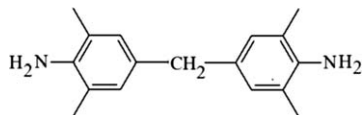
accepted 15 June 2014 Received 29 January 2014;

DOI: 10.1002/app.41191

INTRODUCTION

In a previous article, the broadband dielectric relaxation of several poly(ether imides) containing a segment of poly(oxyethylene) with different chain lengths was investigated.¹ Increasing the flexibility of the ether linkage allows the poly(ether imide) chain to adopt a range of conformations and is reflected in the number and breadth of the observed relaxations. Dielectric relaxation is a useful probe of the effects of changes in the polymer structure on the extent to which the materials may undergo morphological change as the temperature is changed.^{2–20} In this study, a range of anhydride groups are investigated with the structure shown in Figure 1.

This group of polyimides was created by varying R_1 with R_2 held constant and is bis(4-amino-3,5-dimethylphenyl)methane with the structure:



The various structures of R_1 are summarized in Table I. Recently, a number of papers have reported high temperature dielectric properties of polyimides and have shown that changes in the backbone structure influence the α relaxation which is

associated with the glass transition temperature.^{14–20} In most cases, the observation of the dipole relaxation associated with the α relaxation is masked by the effects of conduction losses associated with moisture in the films.

However, poly(ether imides) can exhibit local conformational changes which will influence their flexibility and impacts on the packing density, free volume, and dielectric permittivity. Polyimides are used as thin films in many electronics applications and this study explores the effects of changes in the backbone chemistry on the low temperature dielectric relaxation and their high frequency limiting permittivity— ϵ_{∞}' . In this study, the structure of the backbone is changed so as to impose steric constraints on the extent to which motion can occur.

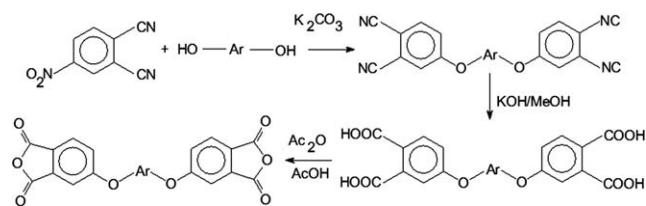
EXPERIMENTAL

Materials

The syntheses of the dianhydrides have been reported previously.^{21–24} The diols incorporated in the dianhydrides which were used to create the poly(ether imides) are listed in Table I.

Synthesis of Polyimides

The bis(ether anhydrides) used in this study were produced by the nitrodisplacement method from the nitrophthalodinitriles by the diol and has been described previously.^{21–24}



The anhydride was reacted with bis(4-amino-3,4-dimethylphenyl) by a conventional in a two-stage solution polymerization and imidization process, as described previously.²⁵ The synthesis involved 1 mmol of diamine being dissolved in 5 cm³ of *N*-methylpyrrolidinone at room temperature and an exact stoichiometric equivalence of dianhydride added with stirring. After standing overnight, the mixtures formed a highly viscous solutions of poly(amic acid)s which was chemically imidized by the addition of 2 cm³ of an equivolume mixture of acetic anhydride and pyrri-

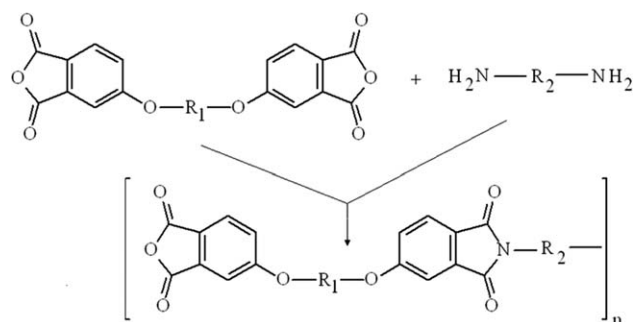


Figure 1. Schematic of the synthetic route used in the production of the polyimides.

dine at room temperature. After leaving for several hours, the resulting polyimides were isolated by precipitation into methanol. Thin films of the polymers were produced by slow solvent

Table I. Diols Incorporated into the Bis(ether anhydride)s to Form the Polyimides

Name	Structure	Code
2,2-Bis(4'-hydroxyphenyl)propane		A1
1,1-Bis(4'-hydroxyphenyl)-1-phenylethane		A2
1,4-Dihydroxy-2-phenylbenzene		A3
2,2-Bis(4'-hydroxyphenyl)hexafluoropropane		A4
Di-(4-hydroxyphenyl)ether		A5
Bis-(4'-hydroxyphenyl)methane		A6
1,5-Dihydroxynaphthalene		A7
5,8-Dihydroxy-1,2,3,4-tetrahydro-1,4-methanonaphthalene		A8
Ether link		A9
2,2-Bis(4-hydroxy-3,5-dimethylphenyl)propane		A10
Bis(4-hydroxy-3,5-dimethylphenyl)methane		A11
4,4'-Dihydroxy-3,3',5,5'-tetramethylbiphenyl		A12

evaporation from polymer solutions (3 wt %) in dichloromethane in flat bottomed Petri dishes (Anumbra). The structures of the anhydride precursors were checked using NMR methods and where appropriate elemental analysis and melting points determined. Details are to be found in previous publications.^{21–24}

The high-molecular weight polyimides were washed with boiling precipitant to remove residual solvent. The transparent, yellow films which were created had a thickness 30–60 μm and were annealed for 3 days at 120°C under vacuum to remove moisture. These films were used for the dielectric analysis.

Density and Differential Scanning Calorimetry (DSC) Measurements

Densities of the cast polyimide films were determined by a flotation method at 25°C using a saturated aqueous solution of K_2CO_3 . The density of the salt solution was measured using an Anton Parr DM60 oscillating digital density meter connected to a DM601 density measuring cell. Measurements were performed in triplicate and the densimeter was thermostated at $25 \pm 0.1^\circ\text{C}$. The glass transition was determined using a Perkin Elmer DSC-2 with a heating rate of 10°C min under nitrogen.

Dielectric Relaxation

Dielectric measurements were carried out using a Novocontrol broadband dielectric spectrometer operating between 0.1 and 6.5×10^4 Hz.²⁶ The Novocontrol spectrometer operates by applying a series of signals of defined frequency to the sample and measuring the amplitude and phase changes which occur as the frequency is scanned. In the initial set up process, the equivalent air capacitance of the sample is determined and subsequent measurements of the cell containing the sample allow the dielectric permittivity to be measured. The phase shift is directly related to the energy dissipation and hence to the dielectric loss. The output parameters from the instrument are the dielectric permittivity and loss as a function of frequency. To achieve maximum electrical contact, aluminum electrodes were coated onto the polymer films using an Edwards E306A coating system. The temperature was controlled by a Linkam CI93 computer interface and a Linkam LNP pump with a liquid nitrogen cooling system. Spectra were recorded at intervals of 10°C from -140 to -60°C . The frequency dependent permittivity $\epsilon'(\omega)$ and dielectric loss $\epsilon''(\omega)$ were fitted to the Havriliak–Negami eq. (1) that allows calculation of the α and β distribution parameters and the characteristic relaxation time τ^{27} :

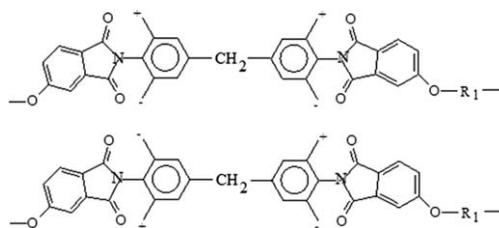
$$\epsilon(\omega)^* = \epsilon_\infty + \frac{\epsilon_0 - \epsilon_\infty}{\left(1 + (i\omega\tau)^{1-\alpha}\right)^\beta} \quad (1)$$

where ϵ_0 and ϵ_∞ are, respectively, the complex and limiting low- and high-frequency permittivities and were initially estimated using plots of the dielectric permittivity against dielectric loss—Cole-Cole plots and ω is the experimental frequency. The values of α and β are frequency-independent, dimensionless constants characteristic of the number and breadth of the relaxation processes involved. For an ideal dipole relaxation process, $\alpha = 0$ and $\beta = 1$. The variation of the characteristic relaxation time, τ as a function of temperature was used to calculate the apparent activation energy using the Arrhenius equation. The fitting of eq. (1) to the experimental parameters allows small changes to be made to ϵ_0 and ϵ_∞ to achieve an optimum fit of the data.

RESULTS AND DISCUSSION

Glass Transition Temperature— T_g and Density Variation

The glass transition temperatures (T_g) of the polymers studied are summarized in Table II. The synthesis creates an imide ring by the reaction of bis-(4-amino-3,4-dimethylphenyl) with the dianhydride and forms a polymer with a semi-rigid central block. The methyl groups in the ortho position to the imide ring twist the phenyl groups out of the plane, which will create for each polymer four possible conformational preferences depending on the relative orientation methyl groups to the plane created by the imide rings: +,−;+,−; −,+,+,−; −,+,+,−; +,−; −; (note shown), −,+,−,+ (not shown). The four conformations will be divided into two energetically degenerate sets: +,−;+,−; −,+,−,+; and −,+,+,−; −,+,+,−;. The existence of two energetically different states indicates the possibility of two closely related but different relaxation processes associated with motion about the N—C bond of the backbone:



Glass Transition Process— T_g

The lowest values of the T_g are observed with A1, A2, and A6. The propane bridge between the phenyl ether rings will impose a twist on the backbone structure and will be further increased when one of the methyl groups is replaced a phenyl group in A2. The twisted backbone structure will inhibit the ability of the polymer chains to pack together. The highest values of T_g are observed when the link is simply an —O— bond or the rigid methyl substituted biphenyl is the linking unit. As with the common central linkage unit, the methyl substitution will introduce the possibility of an additional set of two conformational preferences. As a consequence of the imposed twists in the backbone, A12 has the lowest density which implies that the chains may have difficult packing together; however, the intrinsic rigidity of the backbone inhibits free rotation to a temperature in excess of 420°C, where decomposition becomes apparent. The phenyl substituted dihydroxy benzene linking

Table II. Physical Characteristics of Some Flexible Polyimides

Polymer code	A1	A2	A3	A4	A5	A6
T_g ($^\circ\text{C}$)	245	245	249	258	256	247
Density (g cm^{-3})	1.190	1.194	1.224	1.283	1.235	1.224
Polymer code	A7	A8	A9	A10	A11	A12
T_g ($^\circ\text{C}$)	281	275	>420	274	264	>420
Density (g cm^{-3})	1.225	1.214	1.231	1.140	1.153	1.162

T_g and density at 25°C.

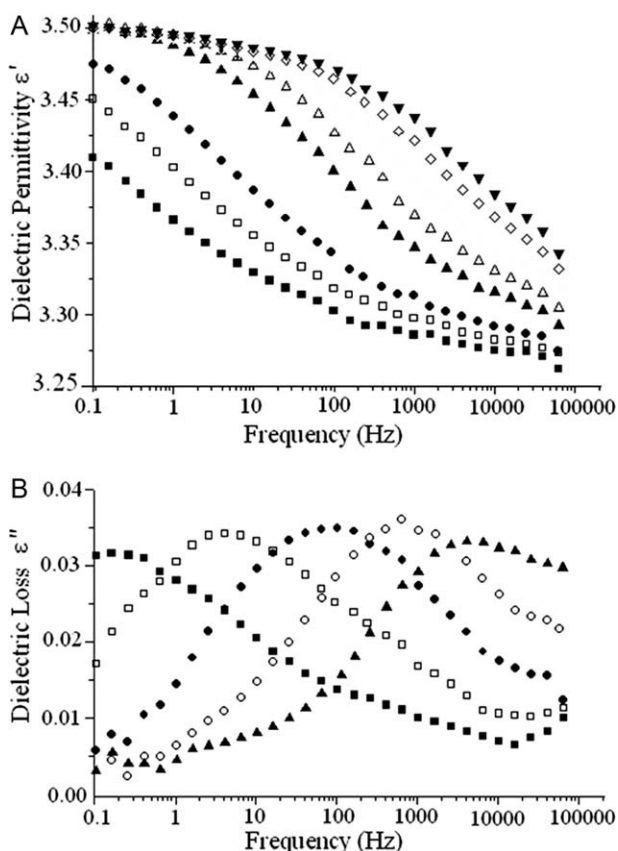


Figure 2. Dielectric permittivity variation with temperature and frequency for A1 (A) and dielectric loss variation with temperature and frequency for A1 (B). Key: temperature variation for (A) ■ -140°C , □ -130°C , • -120°C , ○ -110°C , ▲ -100°C , △ -90°C , ◊ -80°C , ▼ -60°C ; temperature variation for (B) ■ -140°C , □ -120°C , • -100°C , ○ -80°C , ▲ -70°C .

group, A3, exhibits a low T_g , whereas the dihydroxynaphthalene linked polymer A7 has a higher T_g compared with A3 although its density is almost identical. A4 with the hexafluoropropane bridge has a T_g which is slightly higher than A1 but a density which is significantly higher reflecting the higher mass of the six fluorine atoms. The highly substituted phenyl in A8 raises the T_g and has a lower density in comparison with A3 which would be consistent with the inhibiting of neighboring group packing. The highly methyl substituted propane bridged biphenyl A10 has a comparable T_g with A8 but has the lowest density of the polymers studied. The next lowest density is observed with A11 which has a lower T_g consistent with the less restricted methylene compared with the propane bridge in A1. The implication is that both intra- and inter-molecular interactions are influencing the T_g and the packing density in these polymers.

Density Changes in the Series

The polymers studied in this article possess a variety of different side chains which might be expected to inhibit the packing density of the matrix. The highest density is observed with the fluoromethyl substituted bridged A4 which is significant greater than the analogous methyl substituted A1 and reflects the increased strength of the fluorine to induce packing in this matrix. Surprisingly, A2 with a phenyl substitution in the

bridged has a slightly increased density relative to A1 but reflects influence of the out of plane phenyl group on the packing ability. The inhibition of the packing through substitution is reflected in A10 where the methyl substitution in the ring twists the phenyl relative to the phenyl group of the anhydride and lowers the lowest density, most open structure is observed. Removal of the methyl groups from the bridge structure leads to a small increase in the density and its complete removal in A12 leads to a further increase. The polymer containing the oxy-naphthalene groups A7 exhibits a higher density than the 1,2,3,4-tetrahydro-1,4-methanonaphthalene substituted polymer reflecting the ability of the π - π interactions between neighboring groupings to induce closer packing. Removal of the steric hindrance associated with the methyl substitution next to the ether linkage in A11 allows more favorable conformations to be adopted and a higher packing density to be achieved A6. Replacement of the methylene bridge by an ether link further increases the density A5 and A3 exhibits a comparable density with A7.

Low Temperature Dielectric Relaxation

All the polyimides studied exhibit a low temperature relaxation in the frequency range 01 Hz to 10^5 Hz. The shape and precise form of the relaxation changes with temperature and its amplitude varies with nature of the polymer structure. To reduce the amount of data incorporated in the article, the measurements

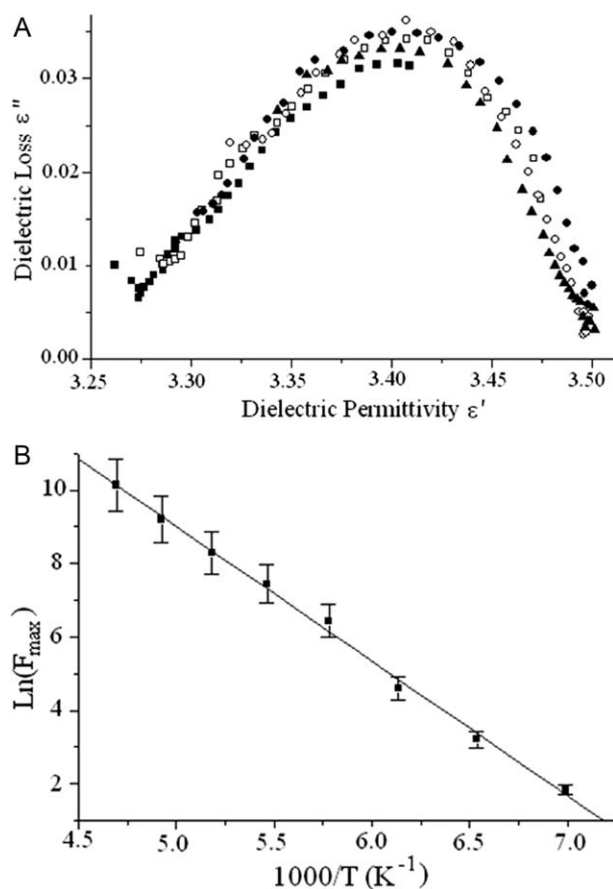


Figure 3. Cole-Cole plots for polyimide A1 (A) and Arrhenius activation energy plots (B). Key of temperature for (A) ■ -140°C , □ -120°C , • -100°C , ○ -80°C , ▲ -60°C .

for A1 will be discussed in detail and the remainder will be presented in a summary form.

Dielectric Relaxation for A1

As an illustration of the dielectric relaxation behavior, the frequency–temperature dependence for polyimide A1 is presented in Figure 2. The dielectric loss peaks reflect the motion of the dipole when subjected to an applied field but do not imply that the dipole is exhibiting free rotation. The conformational changes being detected are restricted to motion between neighboring conformations which do not allow the main backbone to execute large scale motion associated with T_g process but reflect a degree of conformational flexibility. Changes in the substitution pattern of the polymer backbone however can in principle influence the energetic of these dipole processes.

A clear dipole relaxation is observed to move through the frequency window of 0.1 to 10^5 Hz in the temperature range -140°C to -70°C , Figure 2(B). Fitting the Havriliak–Negami eq. (1) to the experimental data, it is possible to calculate the

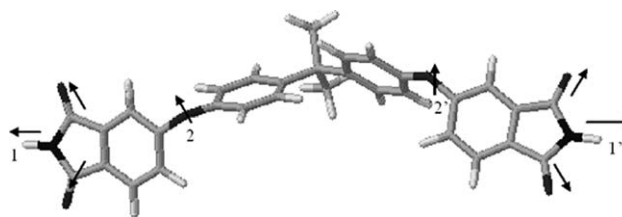


Figure 4. Conformation of a segment of the polymer backbone.

distribution parameters: α and β and the relaxation frequency τ ($= 1/2\pi F_{\text{max}}$). The initial values for the parameters: ϵ_o' and ϵ_∞' are obtained by inspection of Cole–Cole plots, Figure 3(A), in which the variation of the dielectric permittivity— ϵ' is plotted against the dielectric loss— ϵ'' and the values refined in the fitting process. The Cole–Cole plots indicate that the amplitude and the breadth of the relaxation process does not vary significantly with temperature. Assuming that the relaxation process is a thermally activated process then an Arrhenius plots of the

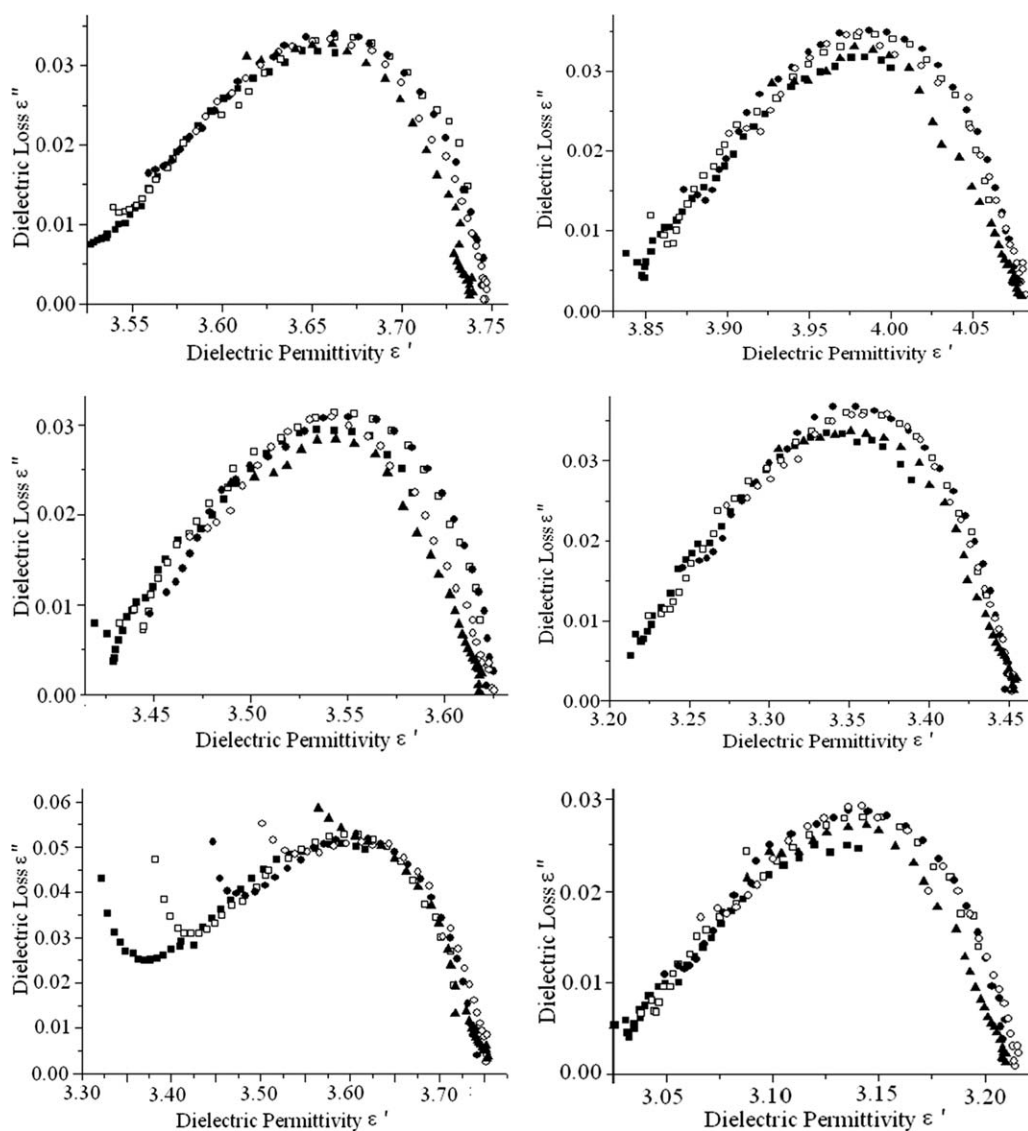


Figure 5. Cole–Cole plots for polymers A2–A12. Key temperatures ■ -140°C , □ -120°C , ○ -100°C , △ -80°C , ▲ -60°C .

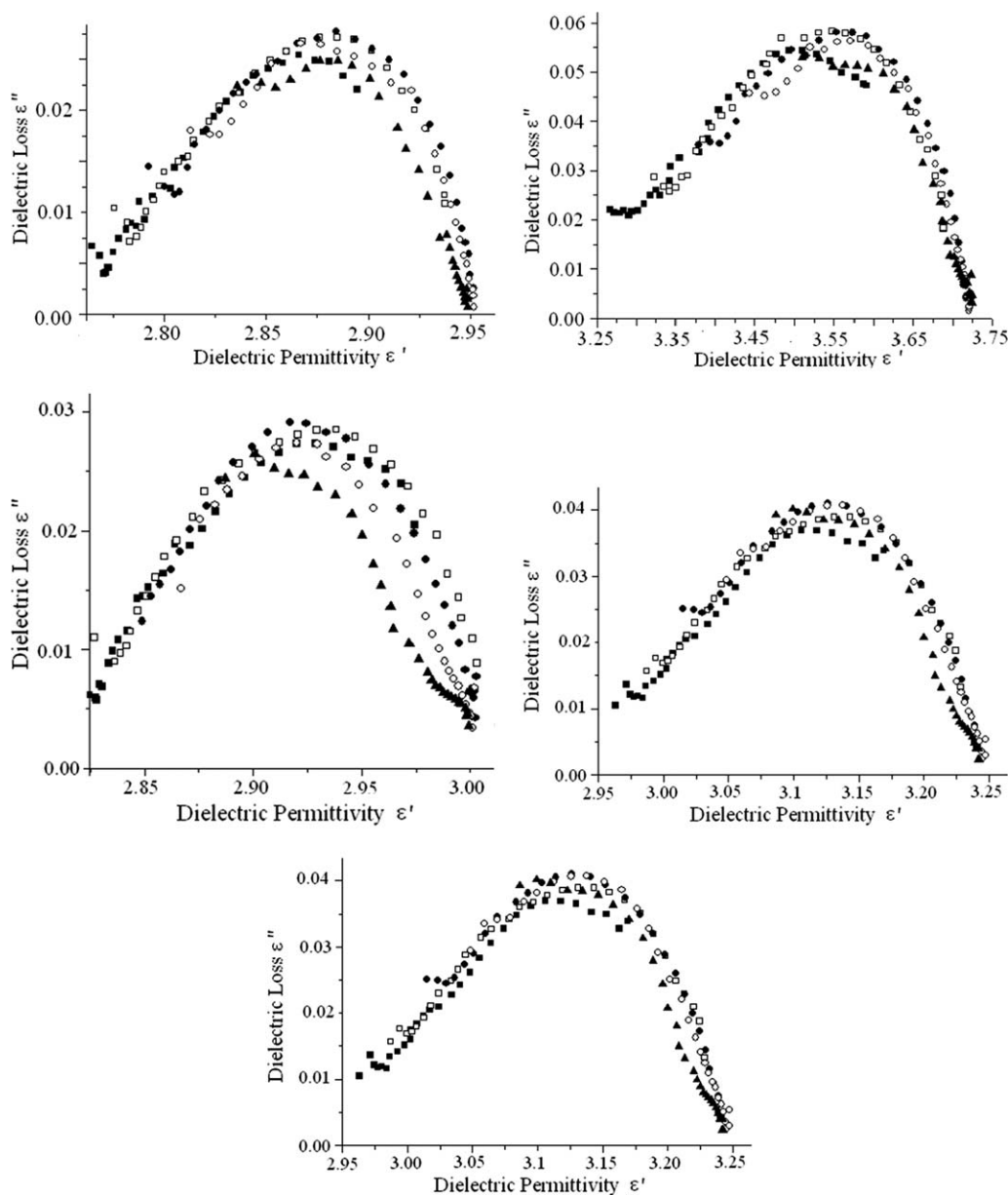


Figure 5. Continued.

variation of $\ln(F_{\max})$ against $1/T$ allows calculation to the effective activation energy for the process, Figure 3(B). The linearity of the plot supports the contention that the relaxation is a simple thermally activated process and yields an activation energy of $30.4 \pm 0.7 \text{ kJ mol}^{-1}$. The values of α and β obtained from a fit of the Havriliak–Negami equation were 0.51 and 0.39, respectively. For an ideal dipolar relaxation, the values of α and β should be 0 and 1. A high value of α and a low value of β is indicative of a coupled–cooperative relaxation processes involving small incremental conformational changes of several bonds to achieve the dipole reorientation process and the effects of the methyl groups associated with the bridging propylene and the central imide segment creates a distribution of backbone conformations. As the temperature is raised, the methyl groups both next to the *N*-phenyl bond and on the bridging propylene

bond will become labile and allow small angle deformations about both the *N*-phenyl and phenyl–phenyl bridge and may be assumed to aid the conformational changes of the polymer backbone. However, the methyl group interactions are sufficiently large to inhibit significant free rotational motion involving the phenyl–phenyl bridge until the glass transition temperature— T_g is reached.

The high value of T_g of this polymer indicates that large scale reorientation of the polymer backbone does not occur until the temperature is raised above 245°C . The relaxation process which occurs below 0°C must be associated with small angle oscillation—librational motions. The restricted nature of the dipole motion is reflected in the small value of the $\Delta\epsilon'$, which is equal to $0.246 (= \epsilon'_0 - \epsilon'_\infty)$ and will involve either or both

Table III. Havriliak–Negami Parameters for the Low Temperature Dipole Relaxation Process

Polymer	α	β	Loss (Max)	ϵ_0	ϵ_∞	$\epsilon_s - \epsilon_\infty$
A1	0.51	0.39	0.035	3.5	3.254	0.246
A2	0.58	0.31	0.034	3.75	3.46	0.240
A3	0.56	0.35	0.035	4.075	3.836	0.239
A4	0.50	0.42	0.037	3.45	3.2	0.250
A5	0.50	0.45	0.031	3.625	3.432	0.193
A6	0.53	0.45	0.030	3.21	3.028	0.182
A7	0.53	0.31	0.052	3.75	3.338	0.412
A8	0.54	0.41	0.028	2.95	2.772	0.178
A9	0.51	0.36	0.058	3.725	3.288	0.437
A10	0.42	0.59	0.029	3.00	2.803	0.197
A11	0.47	0.48	0.041	3.24	2.953	0.287
A12	0.44	0.56	0.040	3.12	2.843	0.277

of the ether and imide linkages. The bridging propane link twists the two phenyl groups out of plane and the methyl groups on the biphenyl will cogwheel with the motion of the carbonyl groups on the imide ring, Figure 4.

Within the imide ring, the dipoles associated with the two carbonyl groups should in principle cancel transverse to the ring but have a component along the polymer backbone which should be cancelled by the matching dipole on the other end of the segment. A resultant dipole will arise as a consequence of distortion of the ring structures and twisting of the chain through interaction with other polymer chains. The ether link will have a definite dipole component transverse to the chain axis, Figure 3 and this would sense co-operative reorientational motion which involves several bonds within the local segment.²⁸ The ortho methyl groups in the diamine will hinder the free rotation of the imide groups introduce a distribution of conformations and constrain any motion to oscillatory—libration rather than full rotation.

Molecular force field calculations²⁹ involving minimization of the energy of the segment produced the structure shown in Figure 4. Molecular dynamic calculations allow the effects of increase in the temperature on the ability of the polymer chain to undergo rotational motion and observations were made up to 300 K. As expected intuitively, the first motions to become active were the rotational motions of the methyl groups which are inactive dielectrically because there is no dipole change on rotational of the group. Further increase in the temperature allowed rocking motions of the central ether linked grouping and at higher temperatures a limited motions about the N—C bond becomes evident. These calculations do not include the very significant effect of π - π and dipole-induced dipole interactions from neighboring chains but give a guide as to the way in which small angular motions can start to allow oscillations of the chain to start.

Dielectric Characteristics of Poly(ether imides) A2–A12

All the poly(ether imides) exhibit similar dipole relaxation processes at low temperature. Rather than presenting the full dielectric permittivity and loss curves, the Cole–Cole plots

are presented in Figure 5. Whilst the general shapes of the Cole–Cole plots are similar, small differences were observed. The Cole–Cole plot for A6 shows the influence of ion conductivity demonstrated by the rise in the dielectric loss on the left-hand side of the plot. The films used had been dried in vacuum for 3 days before the measurements however it is evident that a low level of moisture may have been retained in this film giving rise to a conductivity contribution to the dielectric loss.

The values of α and β are similar for all the polymers, Table III and deviate significantly from the ideal values and imply cooperatively in the nature of the local motion associated with the dipole relaxation. The oscillatory motion involves small angle deformations of several bonds together and do not occur by the movement of a single bond.²⁸ Variations are observed in the magnitude of the dipole relaxation process $\Delta\epsilon$ as measured by the difference between the high and low frequency values of the permittivity $\epsilon_s - \epsilon_\infty$ change for 0.193 for A5 to a value of 0.437 in A9. The latter corresponds to the shortest linkage between the phthalimide moieties and consequently the highest density of dipoles in the polymer. The temperature dependence of the relaxation processes are summarized in the Arrhenius plot, Figure 6. Values of the activation energies for the dipole relaxation are listed in Table IV. The linearity of the activation plots indicates that the dipole relaxation is a thermally activated process and has values range from 23.8 to 31.0 kJ mol⁻¹.

Typically, the activation energy associated with the glass–rubber transition has value which is usually greater than 100 kJ mol⁻¹.^{30,31} The common feature of all these molecules is the dianhydride-diamine central block structure. The groups contained within the dianhydride are clearly changing the activation energy for the dipole relaxation motion but are not in the same order as the T_g . Comparable values of E_a are observed in A1 and A12 whilst the values of their T_g 's are at opposite ends of the range. The lowest activation energy is observed with the least hindered phenyl ether A5, low values being observed with A10, A8, A4 and slightly higher values for A11, A3, A9, A7 and there is not obvious trends with the very significant variation in the extent of steric hindrance being introduced into the chain structure. This would suggest that the relaxation which is cooperative involves oscillatory—librational motion of the central imide unit conformational motion involving the —O— and limited motion about the C—N bond switching between the two possible conformation states probably not being a significant contribution to the relaxation process. Free rotation about the polymer backbone will to a significant extent be restricted by interaction with neighboring polymer chains which will be influenced by π - π , dipole-induced dipole interactions between the chains.

The magnitude of $\epsilon_s - \epsilon_\infty$, Table III is directly related to the magnitude of the dipole involved in the rotational process, which is largest in A9, the simplest of the polymers examined, having a simple ether linkage between the anhydride groups and would consequently have the highest concentration of these moieties. In principle, if the moiety were to exist in isolation and adopt an extended structure then the carbonyl dipoles

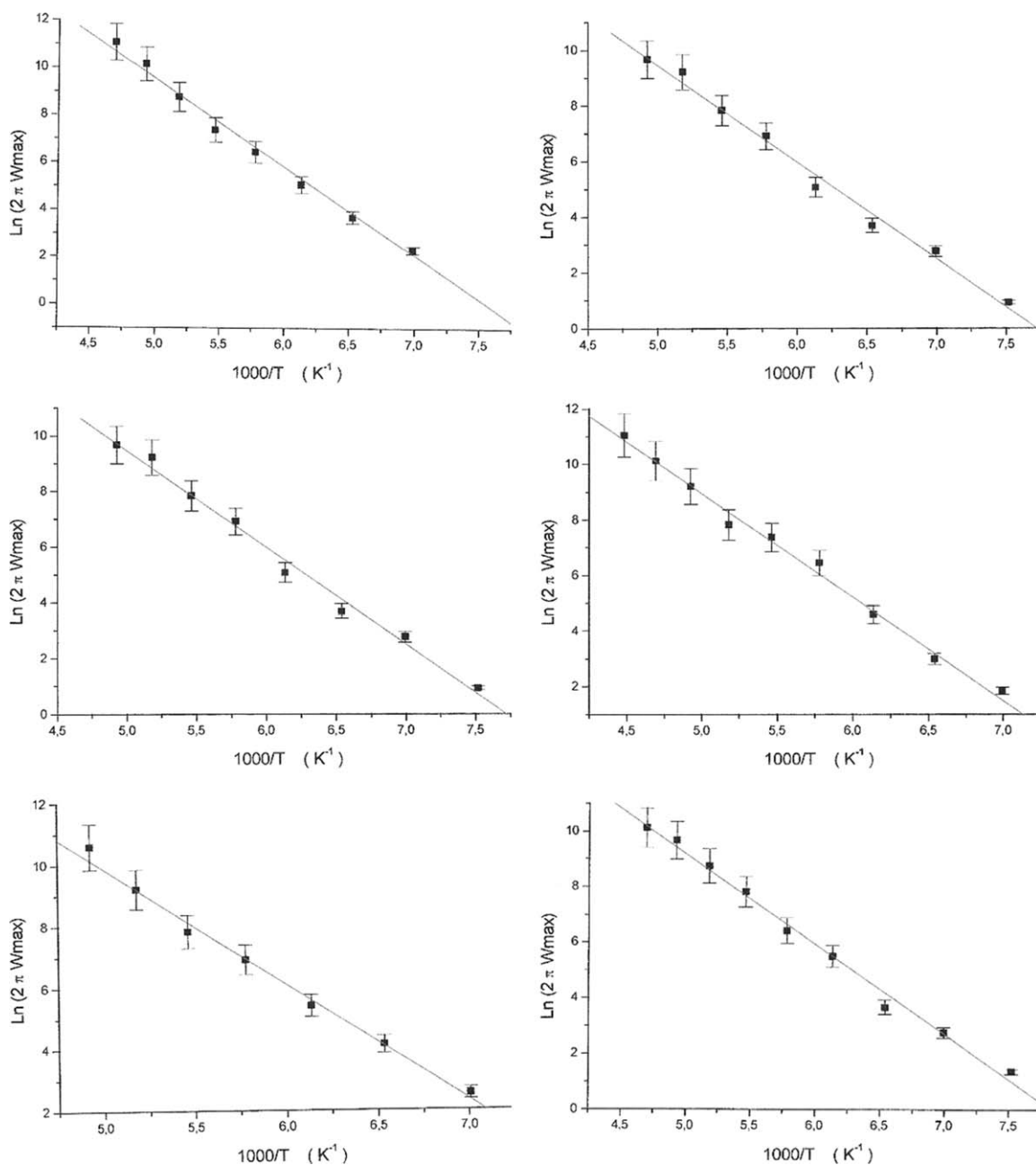


Figure 6. Arrhenius plots for polyimides A2–A12.

would balance each other and the dipole moment would be that of the bridging ether linkage. However, the ether motion can involve coupling with those of other elements in the segment. The ortho methyl groups next the C–N bond hinder the free rotation of the imide groups and constrains any motion to oscillation—libration rather than rotation but switching between the conformations might occur through cogwheel motions of the methyl groups. In the case of A1, the central ether link is replaced by the diphenyl ether which increases the distance between carbonyl groups, reduces the density of dipoles and this is reflected in lower values of $\epsilon_s - \epsilon_\infty$. In the case of A7, the bridging group is the 1,5-dihydroxynaphthalene grouping, which is itself a rigid entity but introduces an element of asymmetry into the structure. Molecular models indicate that

the 1,5-dihydroxynaphthalene group aligns the two imide rings in a parallel configuration allowing the motion of the —O— to achieve a value which is only slightly lower than that observed with the simple phenyl ether. The oscillator strength is lower than that for the simple ether bridge but is still amongst the higher values observed. The sensitivity of $\epsilon_s - \epsilon_\infty$ to the changes in structure is consistent with the assumption that it is motions about the ether–ether link that are responsible for the relaxation process. The introduction of a bulky pendant group will increase the chain–chain separation and reduce π - π and dipole-induced dipole interactions. The bis(4'-hydroxy-3',5'-dimethylphenyl)methane, A11 and the 4,4'-dihydroxyl-3,3',5,5'-tetramethylbiphenyl, A12 exhibit comparable values which indicating that steric interactions close to the ether link influencing both

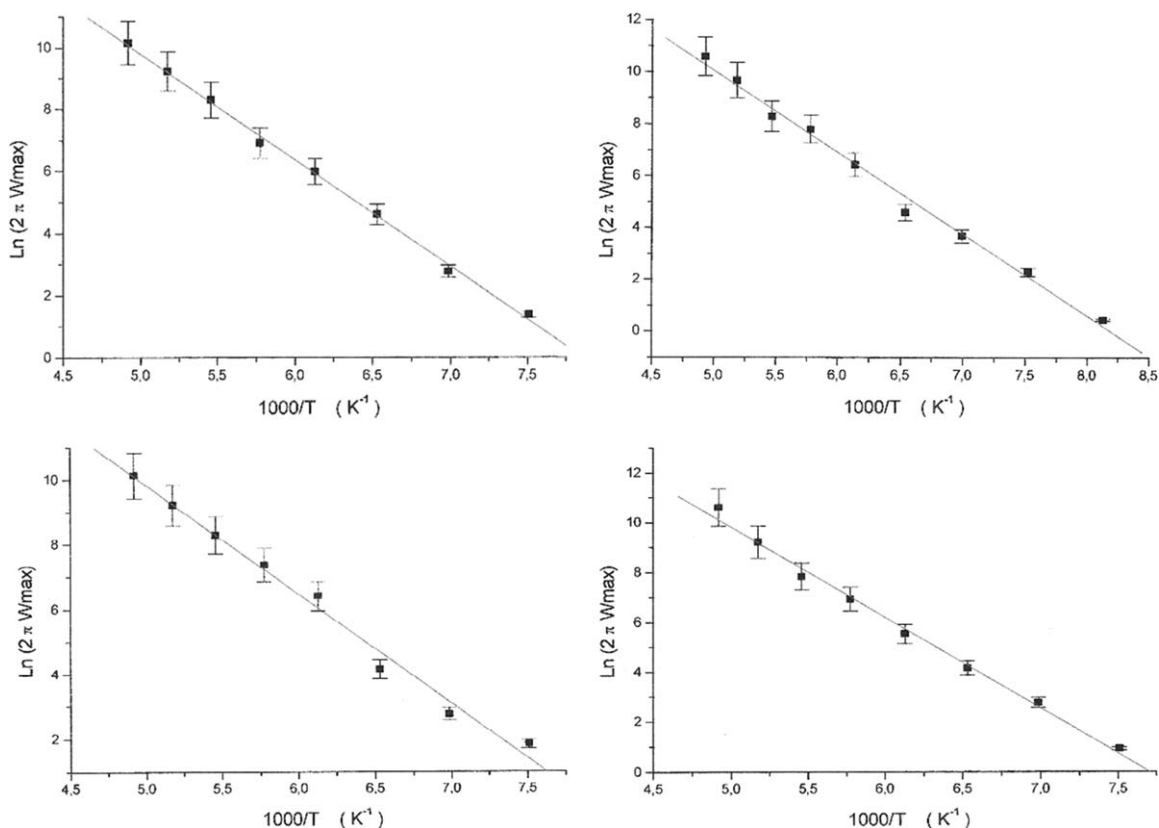


Figure 6. Continued.

the magnitude of the dipole relaxation and its activation energy. The smallest values of $\epsilon_s - \epsilon_\infty$ are observed with the di-4-hydroxyphenylether A5 and bis-(4'-hydroxyphenyl)methane A6 bridging groups. Low values are also observed with the more hindered 2,2-bis(4'-hydroxy-3'5'-dimethylphenyl)methane A10 and 5,8-dihydroxy-12,2,3,4-tetrahydro-1,4-methanonaphthalene A8. Although there have been major changes in the backbone structure, only small changes are observed in the activation energy associated with dipole reorientation, Table IV. The highest activation energy is observed with the A6 and change on the methylene bridge to propylene rather than increasing the activation energy lowers the value by $\sim 2 \text{ kJ mol}^{-1}$. Introduction of sterically hindered groups and pendant groups such as in A1, A2, A4, A9, A10, lead to changes in the value of ΔE_{act} but not in a systematic manner. In conclusion, the values of $\epsilon_s - \epsilon_\infty$ appear to reflect changes in the steric interactions about the ether link but the motion involved is cooperative involving the simultaneous motion of a number of bonds.

High Frequency Limiting Values ϵ_∞

The high frequency limiting value of the dielectric permittivity is determined by the atomic composition of the polymer backbone and its atomic packing density. A plot of the values of ϵ_∞ against the density of the poly(ether imide) films, Figure 7, shows a tendency to increasing values of ϵ_∞ with increasing density, which is what would be intuitively expected; however, there is no simple correlation observed.

Low values of the dielectric permittivity have been reported for 1,3-bis[4-(4-aminophenoxy) phenyl]adamantane with various aromatic tetracarboxylic dianhydrides with values being in the range 2.77 and 2.91, Ref. 2, which is similar to the values observed for A8, Figure 6. The inclusion of the pendant adamantane grouping with increase chain-chain separation but more importantly will change the extent to which π - π and dipole-induced dipole interactions contribute to the limiting value of ϵ_∞ . A low value of ϵ_∞ implies that the extent of the chain-chain interactions has been reduced and this can occur without necessarily reducing the

Table IV. Activation Energy for Dipole Relaxation in the Series A Poly(ether imides)

Polymer	A1	A2	A3	A4	A5	A6
E_a (kJ mol ⁻¹)	30.4 ± 0.7	30.9 ± 0.9	28.8 ± 3.0	26.0 ± 1.0	23.8 ± 0.9	31.0 ± 1.1
Polymer	A7	A8	A9	A10	A11	A12
E_a (kJ mol ⁻¹)	28.9 ± 0.6	26.9 ± 0.8	28.4 ± 0.6	26.1 ± 0.9	27.9 ± 1.3	30.1 ± 1.0

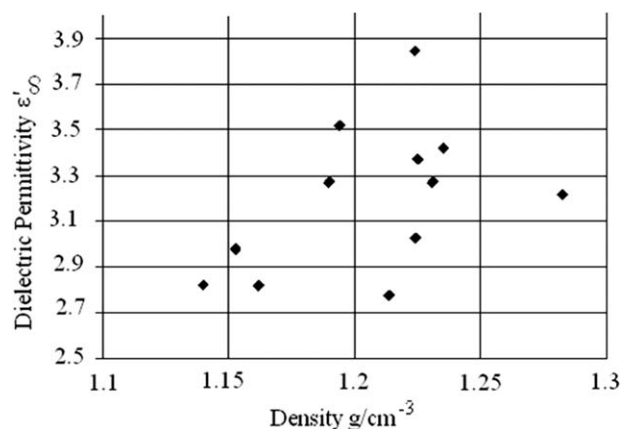


Figure 7. Variation of the high frequency permittivity with density for some poly(ether imides).

overall density. Studies of benzophenone-tetracarboxylic dianhydride with a cycloaliphatic dianhydride namely 1,2,3,4-cyclopentane-tetracarboxylic dianhydride produced values of the dielectric permittivity of 2.97–3.24 depending on the composition of the polymer. Measurements on 4,4'-diaminodiphenylmethane and 3,3'-dimethyl-4,4'-diaminodiphenylmethane with 4,4'-isopropylidenediphenoxy-bis(phthalic anhydride)¹ benzophenonetetracarboxylic dianhydride,² and hexafluoroisopropylidene-bis(phthalic anhydride).^{3–6} The polymers containing the isopropylidene groups gave values of ϵ' of 3.25 and 3.08 which was lower than the related polymers containing the benzophenonetetracarboxylic dianhydride segments which had values of 3.48 and 3.32. It was observed that thermal annealing of the films lead to changes in the values the magnitude of $\Delta\epsilon''$ which decreasing to approximately $1/2$ of their original value on annealing. Annealing has been shown to increase the packing density and inhibits chain motion.

CONCLUSIONS

The low temperature dielectric relaxation is influenced by the chemical structure of the ether linkage in the poly(ether imide)s studied in this article. The higher frequency limiting values of the permittivity increase with the polymer density; however, the values observed reflect the influence of packing density and the presence of nonpolar groupings in the polymer structure. The low temperature relaxation process does not conform to the motion of a simple dipole but is consistent with a more co-operative motion of a number of dipole containing elements.

ACKNOWLEDGMENTS

The support of J.P. and F.S.-M. by the EPSRC are gratefully acknowledged.

REFERENCES

- Eastmond, G. C.; Paprotny, J.; Pauson, A.; Pethrick, R. A.; Santamaria-Mendia, F., submitted.
- de Abajo, J.; de laCampa, J. G. In *Progress in Polyimide Chemistry*; Kricheldorf, H. R., Ed.; Springer: Berlin, **1999**; pp 23–61.

- Chern, Y.-T.; Shiue, H.-C. *Macromolecules* **1997**, *30*, 4646.
- Chern, Y.-T.; Shiue, H.-C. *Chem. Mater.* **1998**, *10*, 210.
- Chern, Y.-T.; Shiue, H.-C. *Macromolecules* **1997**, *30*, 5766.
- Chern, Y.-T.; Shiue, H.-C. *Macromolecules* **1998**, *31*, 5837.
- Chisca, S.; Musteata, V. E.; Sava, I.; Bruma, M. *Eur. Polym. J.* **2011**, *47*, 1186.
- Chisca, S.; Musteata, V. E.; Sava, I.; Bruma, M. *J. Polym. Res.* **2013**, *20*, 111.
- Diaham, S.; Locatelli, M.-L.; Lebey, T.; Dinculescu, S. *Eur. Phys. J. Appl. Phys.* **2010**, *49*, 10401.
- Eichstadt, A. E.; Ward, T. C.; Bagwell, M. D.; Farr, I. V.; Dunson, D. L.; McGrath, J. E. *Macromolecules* **2002**, *35*, 7561.
- Khazaka, R.; Locatelli, M. L.; Diaham, S.; Bidan, P.; Dupuy, L.; Grosset, G. *J. Phys. D: Appl. Phys.* **2013**, *46*, 065501.
- Bacosca, I.; Bruma, M.; Koepnick, T.; Schulz, B. *J. Polym. Res.* **2013**, *20*, 53.
- Ree, M.; Kim, K.; Woo, S. H.; Chang, H. *J. Appl. Phys.* **1997**, *81*, 698.
- Deligo, H.; Saadet Ozgumus, S.; Yalcinyuva, T.; Yildirim, S.; Deger, D.; Ulutas, K. *Polymer* **2005**, *46*, 3720.
- Qu, W.; Ko, T.-M.; Vora, R. H.; Chunbg, T.-S. *Polymer* **2001**, *42*, 6393.
- Comer, A. C.; Kalika, D. S.; Rowe, B. W.; Freeman, B. D.; Paul, D. R. *Polymer* **2009**, *50*, 891.
- Damaceanu, M.-D.; Musteata, V.-E.; Cristea, M.; Bruma, M. *Eur. Polym. J.* **2010**, *46*, 1049.
- Hamciuc, C.; Carja, I.-D.; Hamciuc, E.; Vlad-Bubulac, T.; Ignat, M. *Polym. Adv. Technol.* **2013**, *24*, 258.
- Jacobs, J. D.; Arlen, M. J.; Wang, D. H.; Ounaies, Z.; Berry, R.; Tan, L.-S.; Garrett, P. H.; Vaia, R. *Polymer* **2010**, *51*, 3139.
- Comer, A. C.; Ribeiro, C. P.; Freeman, B. D.; Kalakkunnath, S.; Kalika, D. S. *Polymer* **2013**, *54*, 891.
- Eastmond, G. C.; Paprotny, J. *Polymer* **2002**, *43*, 3455.
- Eastmond, G. C.; Paprotny, J. *Macromolecules* **1995**, *28*, 2140.
- Eastmond, G. C.; Paprotny, J.; Webster, I. *Polymer* **1993**, *34*, 2865.
- Eastmond, G. C.; Page, P. C. B.; Paprotny, J.; Richards, R. E.; Shaunak, R. *Polymer* **1994**, *35*, 4215.
- Eastmond, G. C.; Paprotny, J.; Pethrick, R. A.; Santamaria-Mendia, F. *Macromolecules* **2006**, *39*, 7534.
- Hayward, D.; Mahboubian-Jones, G. M. B.; Pethrick, R. A. *J. Phys. E: Sci. Instrum.* **1984**, *17*, 683.
- Havriliak, J.; Havriliak S. J. *Polymer* **1996**, *37*, 4107.
- Hallary, J.-L.; Lauprete, F.; Monnerie, L. *Polymer Materials*; Wiley: New York, **2011**.
- Molecular Dynamic Calculations, Chem Bio Draw, Perkin Elmer **2012**.
- Fuchs, P. F. J.; Halvor, S.; Hansen, H. S.; Huünenberger, P. H.; Horta, B. A. C. *J. Chem. Theory Comput.* **2012**, *8*, 3943.
- Pethrick, R. A.; Amornsakchai, T.; North, A. M. *Introduction to Molecular Motion in Polymers*; Whittlers Publishing Dunbeth: Caithness, UK, **2011**.